Real-time imaging of on-surface Ullmann polymerization reveals an inhibiting effect of adatoms

Dominik Dettmann,[a,b] Mirco Panighel,[c] Navathej Preetha Genesh,[a] Gianluca Galeotti,[a,†] Oliver MacLean,[a,d] Matteo Farnesi Camellone,[e] Tarnjit Kaur Johal,[a] Stefano Fabris,[e] Cristina Africh,[e] Dmytro F. Perepichka,[f,*] Federico Rosei,[g,*] Giorgio Contini[b,h,*]

a) Centre Énergie, Matériaux et Télécommunications, Institut National de la Recherche Scientifique Department,1650 Boulevard Lionel-Boulet, J3X 1P7, Varennes, Québec, Canada
b) Istituto di Struttura della Materia-CNR (ISM-CNR), via Fosso del Cavaliere 100, 00133Roma, Italy
c) CNR-IOM, Laboratorio TASC, S.S. 14 Km 163.5, Basovizza, 34149, Trieste, Italy
d) Key Laboratory of Functional Materials Physics and Chemistry of the Ministry of Education, Jilin Normal University, Changchun 130103, P. R. China
e) CNR-IOM, Consiglio Nazionale delle Ricerche-Istituto Officina dei Materiali, c/o SISSA, via Bonomea 265, 34136 Trieste, Italy
f) Department of Chemistry, McGill University, 801 Sherbrooke Street West, H3A 0B8, Montreal, Québec, Canada
g) Department of Chemical and Pharmaceutical Sciences, University of Trieste, Via Giorgeri 1, 34127 Trieste (Italy)
h) Department of Physics, University Tor Vergata, via della Ricerca Scientifica 1, 00133 Roma, Italy

†) Present address: Deutsches Museum, Museumsinsel 1, 80538 Munich, Germany

*Corresponding authors email: dmytro.perepichka@mcgill.ca, federico.rosei@inrs.ca, giorgio.contini@ism.cnr.it

ABSTRACT

Ullmann coupling is a widely used reaction for the on-surface growth of low-dimensional carbon nanomaterials. The irreversible nature of this reaction prevents 'self-healing' of defects and detailed knowledge of its mechanism is therefore essential to enable the growth of extended ordered structures. However, the dynamics of the Ullmann polymerization remain largely unexplored as coupling events occur on a time-scale faster than conventional scanning probe microscopy imaging frequencies. Here, we reveal the dynamics of these surface events using high-speed variable temperature scanning tunneling microscopy (STM) (10 frames per second). Performing the measurements at the on-set reaction temperatures provides an unprecedented description of the evolution of organometallic (OM) and covalent surface species during Ullmann polymerization of para-dibromobenzene on Cu(110). Our results demonstrate the existence of an intermediate OM phase with Cu adatoms that inhibits the polymerization. These observations now complete the picture of the pathways of on-surface Ullmann polymerization, which include the complex interplay of the phenylene moieties and metal atoms. Our work demonstrates the unique capability of high-speed STM to capture the dynamics of molecular self-assembly and coupling.

INTRODUCTION

On-surface synthesis is an established tool for the preparation of low-dimensional organic structures with unique properties.[1-3] The main approaches reported so far include condensation reactions such as Schiff-base coupling[4, 5] or boronic acid condensation[6], and C-C coupling reactions that proceed through organometallic intermediates such as Glaser coupling or Ullmann coupling.[7-12] In the former reactions, the surface acts as a passive template facilitating the growth of two-dimensional (2D) structures. The latter reactions are carried out on transition metal surfaces, which also act as a catalyst activating the functional groups.[13, 14] Though on-surface synthesis is very effective in the case of graphene nanoribbons, achieving polymerization on a length scale of even 100 nm with controlled density of defects is extremely challenging, especially for 2D polymers.[1, 7, 15, 16] Defect formation mechanisms lie in the complex interaction between surface, adatoms and reacting molecules.[17]

Previous studies employing various techniques have provided valuable insights into the reaction mechanism, yet were not able to capture the complete picture. Low-temperature measurements offer exceptional imaging of on-surface structures via scanning tunneling microscopy (STM) and non-contact atomic force microscopy (nc-AFM) measurements.[18-21] However, the low-temperature conditions do not allow for the direct study of thermally-activated reactions. The kinetics of on-surface polymerizations typically occur at higher temperatures and are commonly investigated by spectroscopic means.[22-28] The effect of the surface on the order of the resulting systems was studied via systematic Monte Carlo simulations that suggested that a high rate of monomer diffusion relative to coupling is required to achieve large ordered domains of 2D polymers.[29] This conclusion was experimentally supported by kinetic measurements of Ullmann coupling via temperature programmed X-ray photoelectron spectroscopy (TP-XPS).[22, 24, 30] These measurements demonstrated the feasibility of both diffusive and topotactic driven reactions.[22]

The intermediate reacting species incorporate metals atoms during the on-surface Ullmann reaction, and previous work has demonstrated that the mobility of these species is key in forming ordered covalent bonded polymers.[29] The stabilizing metal atoms can originate from freely roaming metal adatoms or surface atoms.[31] The covalent organometallic bond with a free adatom could be significantly stronger due to increased coordination with the substrate and therefore adatoms can have a key role in determining the reaction dynamics. The impact of these adatoms on the reaction pathway as it plays out at elevated temperatures is unclear and requires variable temperature STM measurements to capture these effects. However, due to the high mobility of molecules on surfaces, especially at temperatures close to the reaction on-set, conventional scanning frequencies cannot capture these transient states.

High-speed STM represents a powerful technique to study the dynamics of molecular self-assembly and polymerization with molecular resolution, as its millisecond-scale acquisition time makes it possible to capture transient states throughout the course of diffusion and reaction.[32-34] In previous studies, this technique was applied to study the stability of metal surfaces at electrochemical interfaces and revealed the formation and migration of subsurface species,[35] surface reconstructions induced by hydrogen evolution[36] and diffusion of ions on the surface.[37-39] This technique could address crucial open questions such as the dynamics of self-assembled domain growth or whether polymerization proceeds through a step- or chain-growth mechanism; i.e, if monomers couple to dimers which in turn couple to oligomers or if individual monomers couple to a growing chain.[40]

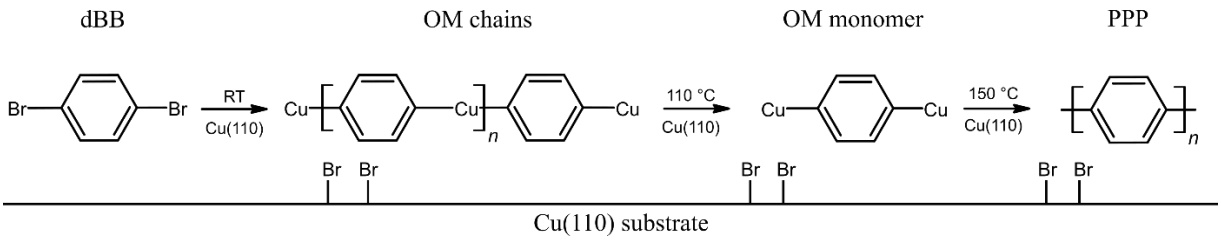

Scheme 1. On-surface Ullmann reaction of 1,4-dibromobenzene (dBB) on Cu(110) at sub monolayer coverage.

The Ullmann-like coupling of 1,4-dibromobenzene (dBB) on Cu(110) provides an excellent model system for a high-speed STM study of on-surface polymerization. **Scheme 1** shows the reaction mechanism of the on-surface polymerization of dBB on Cu(110). Upon adsorption on the substrate, the aryl halide dehalogenates and forms organometallic (OM) chains, in which phenylenes are linked by Cu atoms. Annealing at 110 °C transforms the OM chains into OM monomers, in which each phenylene is individually saturated by Cu atoms. Further annealing at 150 °C promotes the polymerization of these OM monomers into poly-*p*-phenylene (PPP). Despite the simplicity of the molecule, the polymerization process is intriguingly complex and involves different intermediate states. It has been demonstrated that a stable 2D organometallic network forms before the final C-C coupling into PPP chains at submonolayer coverage.[41] However, the reason for the formation of a 2D organometallic network given the 1D functionalization of the precursor was previously unknown.

Here, we report the first high-speed variable temperature STM study of the Ullmann polymerization on Cu(110) performed at temperatures close to the reaction on-set. We reveal the growth dynamics of two meta-stable OM phases constructed from individual phenylenes saturated by Cu adatoms (OM monomer) at 110 °C. High-speed STM measurements show the dynamic exchange of OM monomers between the two phases. At 150 °C, PPP formation is observed from randomly diffusing OM monomers and occurs along the [1 -1 0] surface direction. The polymerization follows a linear growth mechanism, in which monomers attach to the end of the growing PPP chain. We provide experimental mechanistic insights into the dynamic formation of organometallic phases as the Ullmann reaction proceeds at different temperatures and identified an intermediate, isolated OM monomer, that diverges from the classic Ullmann reaction pathway. Our results demonstrate the unique capability of high-speed STM to study the dynamics of on-surface reactions with molecular resolution and should spark interest in studying relevant catalytic reactions such as C-H activation or CO_2 reduction using high-speed STM.

RESULTS

To gain insights into the molecular dynamics involved in Ullmann coupling and the influence of intermediate phases on the final product, we investigated the structures on the surface held at different temperatures using STM. Dosing 0.5 ML of dBB on Cu(110) held at RT yields one-dimensional (1D) OM chains along the [1 -1 ±1] surface directions that consist of alternating Cu atoms originating from the surface and phenylene groups with a periodicity of 0.69 ± 0.03 nm (**Figure 1a**), as previously reported.[42, 43] Annealing to 110 °C leads to the formation of two intermediate organometallic self-assemblies (**Figure 1b,c**). A 2D OM network emerges that is

made of individual phenylene moieties saturated by two Cu adatoms (OM monomer, **Scheme 1**), forming a square with a distance between two Cu adatoms connected to the same phenylene of 0.71 ± 0.03 nm, as previously reported[41] (**Figure 1b**). Moreover, these OM monomers also self-assemble along the [0 0 1] direction forming 1D structures with a periodicity of 1.11 ± 0.06 nm (black line in the inset of **Figure 1c**). STM simulation supports that this 1D structure is made of periodically aligned OM monomers (**Figure S1**). Small features in between the rows of OM monomer are tentatively attributed to co-assembled bromine atoms (**Figure 1c**). At 110 °C, we solely observe the self-assembled structures formed by the OM monomers, which suggests that these OM monomers are the intermediate product. The absence of any OM chains at this elevated temperature is coherent with previous TP-XPS work.[41] The origin of the incorporated Cu adatoms is different between the OM chain (**Figure 1a**) and the OM monomer structures (**Figure 1b,c**) as previously shown.[22, 23, 42] Whereas the former lifts surface bound atoms slightly out of its equilibrium position,[23, 42] the latter interacts with Cu adatoms.[31, 41]

At 150 °C, neither the 1D nor 2D self-assembly of OM monomers are observed. The structures dissolve and instead at this temperature, we observe the formation of the covalent PPP chains (**Figure 1d**). The measured periodicity of 0.48 ± 0.02 nm is in agreement with what was previously reported (0.44 ± 0.02 nm).[42] The occurrence of two OM self-assemblies acting as reservoirs for intermediate OM monomer species at 110°C, bridging the temperature gap between the RT OM chain and the PPP polymer product at 150°C, is unexpected. We note that the reaction onset temperatures observed in this work under isothermal conditions are slightly different from previous TP-XPS works[24, 41]; this is in line with the known dependence of the reaction onset temperature on the heating rate.[24] To understand what drives the formation of different geometries along the on-surface Ullmann reaction pathway and the role of the different OM phases in the reaction mechanism, we carried out high-speed STM measurements (0.1 s per image) at 110 °C and 150 °C.

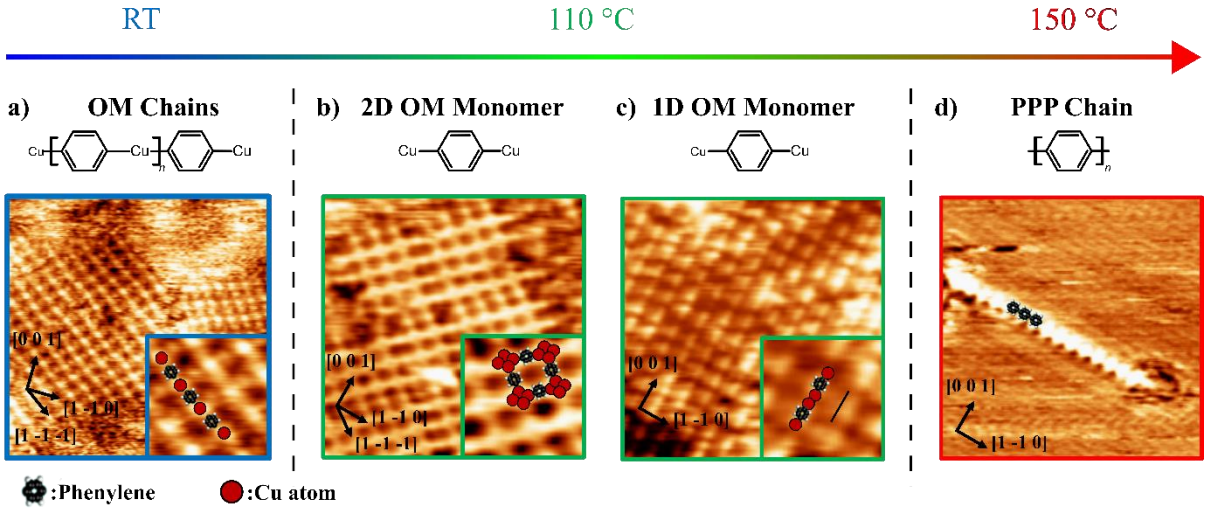

Figure 1. Variable temperature STM measurements of dBB on Cu(110). a) Dosing 0.5 ML of dBB on Cu(110) held at RT yields OM chains. b,c) Annealing at 110 °C triggers the formation of OM monomers, which assemble in 1D and 2D OM networks. d) Annealing at 150 °C enables polymerization and PPP chains along [1 -1 0] are observed. The superimposed schemes show the building block of each phase. Insets provide information on the adsorption geometry. Periodic structures of the adsorption geometry in a), b) and c) can be found in Fig. 3a, Fig. S8, Fig. S1, respectively. Images: a) 13.1 x 13.1 nm^2, -0.2 V, -0.6 nA b,c) 13.1 x 13.1 nm^2, 0.2 V,

0.6 nA, d) 9.2 x 9.2 nm^2, -1.0 V, -1.0 nA. Insets: a) 2.5 x 2.5 nm^2, b) 3.2 x 3.2 nm^2, c) 3.4 x 3.4 nm^2. Measurements taken with conventional scanning speeds (>30 s per frame) and with the substrate held at RT (a), 110 °C (b,c) and 150 °C (d).

Our variable temperature STM investigation shows that there is an intermediate temperature interval during the on-surface Ullmann reaction at which two different metastable phases constructed from the same OM monomer co-exist. We employed the high-speed scanning mode to observe the diffusion, construction and dissolution of these phases. **Figure 2** shows a sequence of STM frames at 110 °C that capture the formation of the 2D OM Monomer network as the 1D OM Monomer structure along the [0 0 1] direction vanishes. We observe the 2D OM Monomer network in the upper part of the frame and the 1D OM Monomer structure in the lower part (indicated by a blue box) in **Figure 2a**. After 0.1 s, the 1D phase has collapsed and released individual OM monomers (**Figure 2b**). These OM monomers can roam the surface and attach to the 2D OM Monomer network, as shown by the extension of the bottom row and the right column of the 2D OM Monomer network after 0.2 s (white arrows in **Figure 2c**). Furthermore, we observe bright dots in the STM image, which are attributed to randomly diffusing Cu adatoms (marked by red-yellow dots in **Figure 2c**) as their height is similar to the linear Cu adatoms in the network (**Figure S2**). At the bottom of **Figure 2c**, an approaching OM monomer (indicated by a black arrow) attaches to the right column of the 2D OM network (indicated by a white arrow in **Figure 2d)**. This series of STM images capture the elementary steps of the growth of the 2D OM monomer network: the rotation of the OM monomers, the diffusion to the network and attachment to the network. In **Figure 2e-f**, the continuous growth of the network is followed over a longer time (5.5 s). This phase transformation is reversible as OM monomers are also seen to be released from the 2D OM Monomer network and reconstruct the 1D OM Monomer structure as shown in **supplementary movie 1** (**SM 1**). While the STM measurement could potentially affect the surface reactions, we consider it to be unlikely due to the usage of conventional scanning parameters and a significantly reduced tip-sample interaction time.

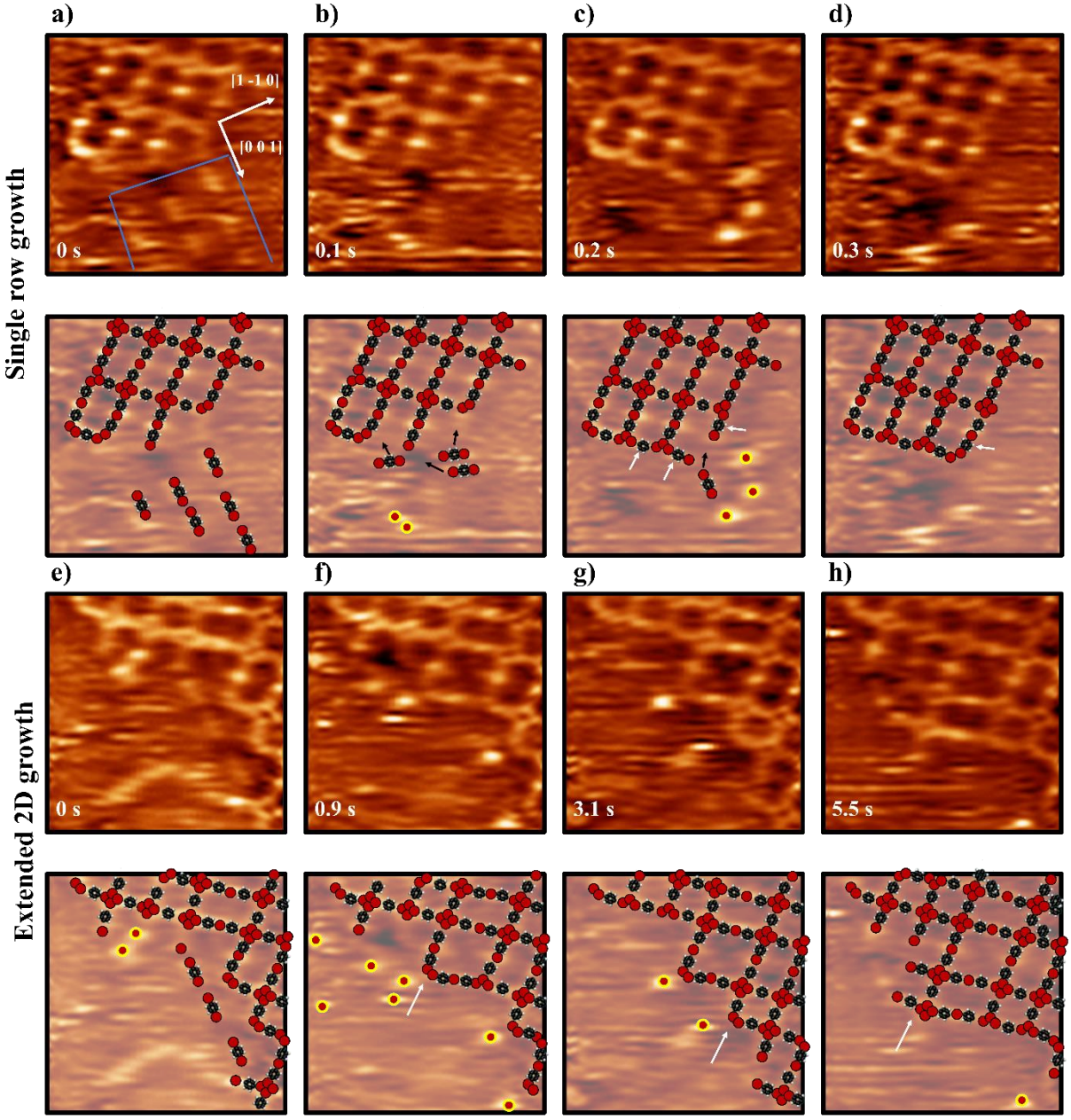

Figure 2. High-speed STM measurements at 110 °C showing the growth of the 2D OM Monomer network. a-d) Growth of a single row of the 2D Monomer network within 0.3 s. In the bottom of a) the OM monomers are present and after 0.1 s collapsed to interact with the 2D network. e-h) Extended growth of the 2D Monomer network over 5.5 s. Below each STM image is a schematic of the STM image to visualize the change during the sequence. Molecular models are superimposed over both static and mobile features. Black arrows indicate diffusing units and white arrows show the addition of units compared to the previous frame. Images size: 8.6 x 8.6 nm^2. -0.2 V, 2.4 nA.

Next, we focused on recording the polymerization process and determining the mechanism through which PPP chains are formed. **Figure 3** shows two series of STM images at 150°C that provide insights into the polymerization and growth process. High-speed STM measurements suggest that the polymerization process is driven by the addition of randomly diffusing OM monomers that bind to the end of an existing oligomer. In the upper row STM sequence, the attachment of single phenylene to a growing oligomer chain is shown (**Figure 3a-d)**. In **Figure**

3a, a phenylene is approaching the oligomer chain. Within the next 0.2 s, it aligns with the surface direction of the oligomer (**Figure 3b,c**) and couples 0.1 s later (**Figure 3d**). **Figure 3e-h** shows extended growth of the PPP chain along the [1 -1 0] surface direction (**Figure S3** and **movie SM 2** show consecutively taken STM images). The energy barrier for diffusion of OM monomers along this surface direction is calculated by DFT to be between 0.10 eV and 0.70 eV depending on the orientation (**Table S1, Figure S4)**. While diffusion along the [1 -1 0] surface direction exhibits the lowest energy barriers, diffusion is not restricted along this direction due to the moderate activation energies from 0.90 eV to 1.20 eV (**Table S1, Figure S4**). We estimate an OM monomer diffusion velocity of 4 nm/s based on the movement observed in Figure 3a-d, which is in good agreement with a theoretical values (5.8 nm/s to18 nm/s) obtained through the activation energies calculated by NEB-DFT (SI Section 4). The growth process is exclusively driven by the addition of phenylenes to the end of the chain rather than a step-growth polymerization involving the coupling of oligomers or a direct transition from the OM chain to the PPP chain.

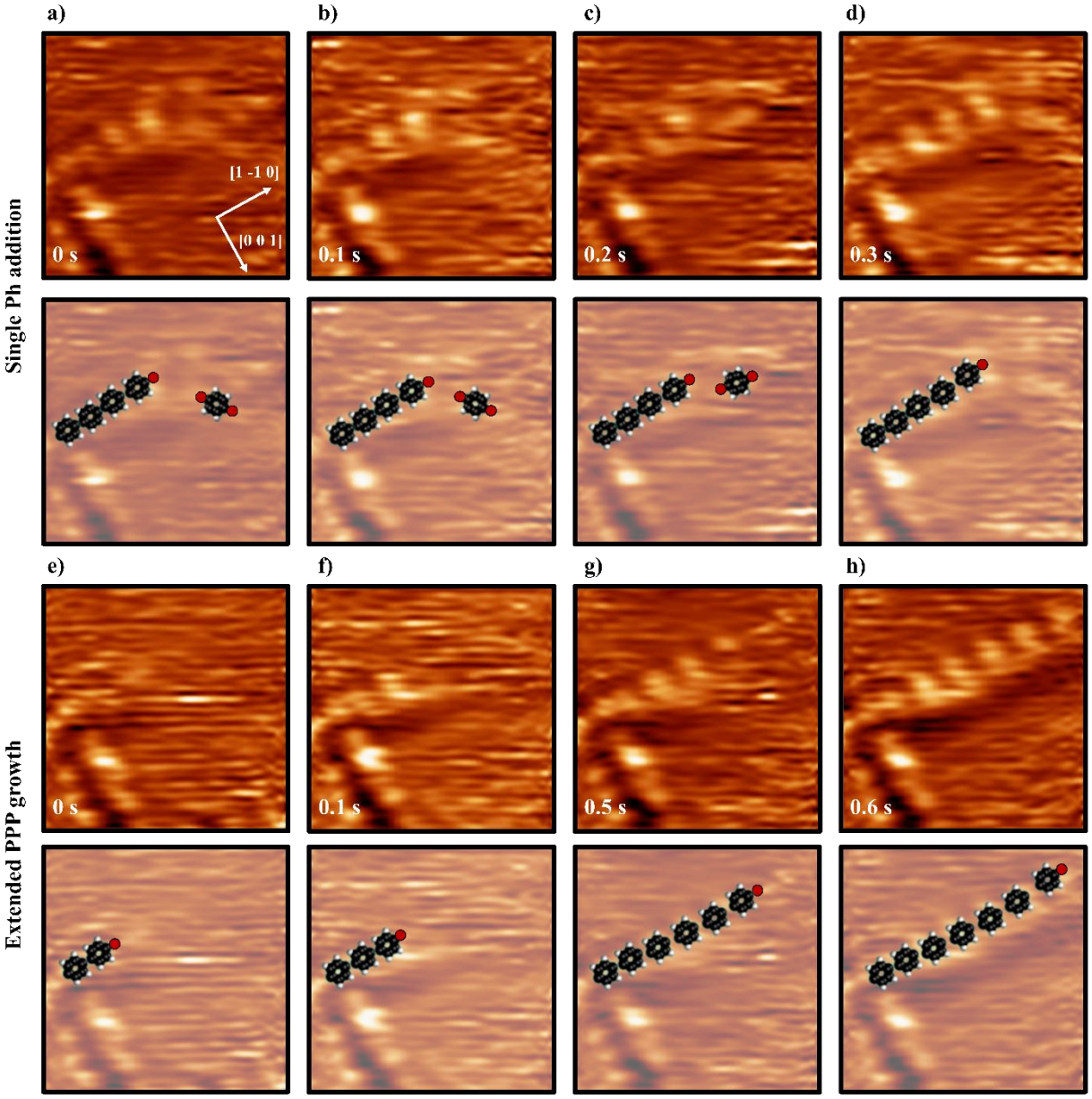

Figure 3. High-speed STM measurements at 150 °C of the growth of PPP chains. a-d) Addition of a single phenylene to a small PPP chain within 300 ms. Red dots are Cu atoms. e-h) Extended

growth of a PPP chain. The black arrows in a-d) indicate the movement of the coupling phenylene. Below each STM image is a schematic of the STM image to visualize the change during the sequence. Molecular models are superimposed over both static and mobile features. Images size: 3.0 x 3.0 nm^2. 0.6 V, 5.5 nA.

DISCUSSION

The results described above show that the 'trapping" of dehalogenated molecules by diffusing Cu adatoms is the dominant interaction limiting the rate of Ullmann coupling on Cu(110). The source of metal atoms involved in OM structures is elusive.[31, 42] Two possibilities are commonly discussed in this context, the incorporation of lifted surface atoms or preexisting adatoms to the OM structures. Although the formation energy of adatoms from the perfect flat surface is large (0.77 eV, **Figure S5**), the formation energy from ledges on Cu(110) is only 0.014 eV per atom, making the ledges a significant source of adatoms.[44] Therefore, it is expected that diffusing Cu adatoms are available to interact with the phenylenes during the reaction at 110 °C.

To understand the thermodynamic picture of the Ullmann reaction mechanism of phenylenes and its intermediates on Cu(110), we computed the formation energies of OM chains, OM monomers and dimers (**Figure 4**). We found a thermodynamically favorable trend for the transition of OM chains to adatoms-terminated OM monomers of 0.28 eV per phenylene. OM monomers terminated with Cu atoms lifted from the surface are significantly more endothermic (>1 eV, **Figure S6**). A discussion about the relative stability between OM monomers packed in the 1D or 2D assembly is presented in SI section 7 and 8. We suspect that a kinetic effect related to the availability of Cu adatoms confines the system at RT in the OM chain configuration, in which phenylenes are stitched together via lifted surface atoms. Increased thermal energy at 110 °C raises the density of Cu adatoms and the more stable OM monomers are formed (Figure 4b). Further annealing to 150 °C favors polymerization and forms the covalently-linked phenylenes, which are stabilized by 0.76 eV per phenylene compared to OM chains (Figure 4c).

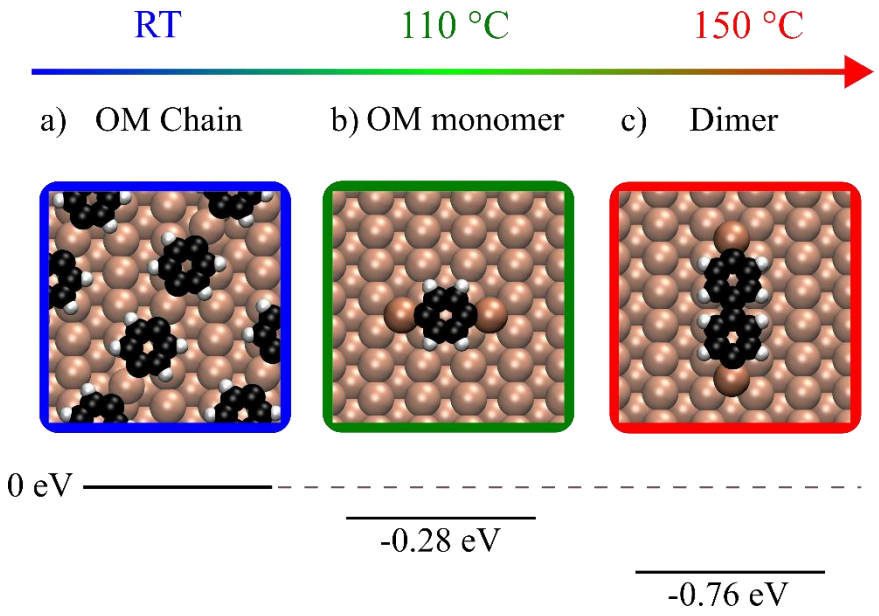

Figure 4. Thermodynamic picture of the stability of different surface species during the temperature evolution. The formation energies for different structures are calculated with

respect to the energy of the OM chains observed at RT (-4.69 eV per phenylene). Positive (negative) values refer to less (more) stable structures. Light and dark brown spheres are Cu surface atoms and adatoms, respectively.

The reaction dynamics of the Ullmann polymerization have been subject to numerous computational studies, but lacked direct experimental evidence. Several scenarios for the polymerization reaction have been proposed.[22, 45] These are commonly based on assumptions from the initial and final state STM images and TP-XPS, and assume the C-C coupling proceeding either directly from the OM chain intermediate[22] or dehalogenated monomers stabilized by surface atoms.[24] However, our measurements demonstrate that the reaction starts from the monomers stabilized by Cu adatoms (OM monomers) and not surface atoms. This reaction step is in agreement by previous TP-XPS measurements, that show no signs of additional species between the OM monomers formed at 110 °C and PPP chains.[41] These critical new details of the Ullmann polymerization obtained through high-speed variable temperature STM enable improved NEB modelling of the reaction and shed light on the elementary steps of the reaction beyond the temporal resolution of the high-speed measurements.

Here, we model the polymerization reaction starting from two OM monomers along the [1 -1 0] surface direction (**Figure 5**). In the first three reaction steps (**Figure 5**), two OM monomers (**1**) are linked into an OM dimer along the [1-1 0] direction by ejecting a Cu atom. In the first step, the bottom unit rotates towards the [1 -1 -1] direction with a barrier of 0.69 eV (**2**). Next, the bottom OM monomer rotates towards the [1 -1 0] direction while ejecting its Cu adatom to connect to the Cu adatom of the top OM monomer. As a result, a metastable OM dimer is formed and the ejected Cu atom resides in the neighboring fourfold hollow position (**3**). The latter can diffuse towards the neighboring fourfold hollow site to further stabilize the intermediate state (**4**). These reaction steps are likely reversible as the forward and backward reaction exhibit similar barriers of 0.57 eV (2→1), 0.59 eV (3→2) and 1.09 eV (4→3). The following C-C coupling along [1 -1 0] direction is the rate-determining step, with an activation energy of 1.07 eV and a change in enthalpy of 1.5 eV. The coupling is accompanied by a simultaneous ejection of the bridging Cu adatom into the fourfold hollow site below the formed biphenylene (**5**). Diffusion of this Cu adatom to the adjacent fourfold hollow site further stabilizes the structure by 0.08 eV (**6**).

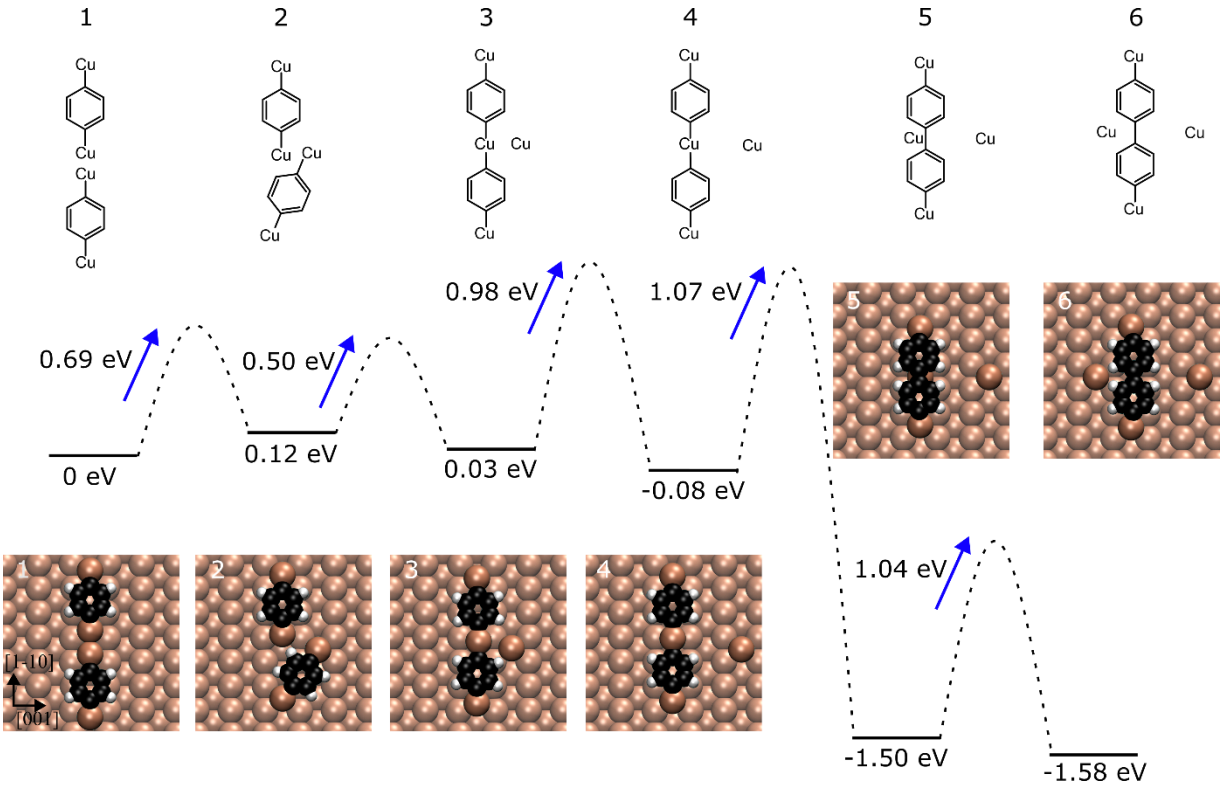

Figure 5. Transition state pathway analysis of the OM monomer polymerization reaction. The reaction pathway is to scale and the numbered states correspond to the stable states found in between separate NEB calculations. The numbered skeleton models illustrate the change between states towards polymerization and refer to the DFT optimized cells. Light and dark brown spheres are surface Cu atoms and adatoms, respectively.

We show that even for a relatively simple molecule, the reaction pathway can be very intriguing; the complexity lies in the variety of interactions between the metal and the dehalogenated monomers, which controls the pathway of the coupling reaction. Standard STM measurements provide information on the initial and final state, but are limited in their insights in possible reaction intermediates.[23] The initial state of OM chains and the final state of PPP chains may suggest that the polymerization occurs via reductive elimination along the chain. However, the observed dissolution of the initial OM chains and the construction of two intermediate phases reject such a mechanism and makes it significantly more difficult to predict the polymerization process. Only high-speed STM measurements performed at the reaction temperature allow for an accurate description of the C-C coupling process.

We demonstrate that the Ullmann-type polymerization can occur through the addition of single reactants to a growing domain. The identification of this polymerization mechanism, compared to a step-growth mechanism, is especially important for growing large domains of two-dimensional polymers as it avoid the formation of oligomers. The oligomers formed by C3 symmetry molecules do not necessarily have the symmetry or shape of the final product. Due to this unavoidable defects might be introduced into the lattice when oligomers of mismatching shape couple. A gradual growth through the single addition of monomers at the edge of the growing domain can avoid this type of defect formation and possibly provide improved thermodynamic control. Such growth could be achieved through avoiding the formation of densely packed structures.[1,15]

Beyond intermolecular reactions, the involvement of metal adatoms in intramolecular reactions such as cyclodehydrogenation is largely based on calculations.[46] Our measurements provide evidence of available Cu adatoms on the surface to an extent at which the reaction diverts into a phase of individual metal-saturated species. High-speed variable temperature STM experiments open a path towards direct experimental description of the reaction dynamics occurring during surface reaction, enabling the identification of reaction intermediates and their participation in the reaction mechanism as well as allowing the epitaxy between reactants and substrate as the reaction occurs to be determined. In turn, the improved experimental description enables DFT calculation with increased confidence.

CONCLUSIONS AND PERSPECTIVES

We experimentally observed the interplay between Cu adatoms and phenylenes in driving the on-surface Ullmann polymerization reaction. A precise description of the polymerization reaction is key to develop strategies to enhance the synthesis of ordered covalent surface structures. By means of high-speed variable temperature STM, an intermediate regime at 110 °C was identified, in which phenylenes are saturated by two Cu adatoms as a result of the increased number of Cu adatoms on the surface. Within this regime, polymerization is inhibited and organometallic self-assemblies dominate. Further annealing provides thermal energy to go beyond the organometallic regime and enables the polymerization via C-C coupling. We also found that PPP formation occurs along a single surface direction via reductive elimination of Cu from the ad-atom bridged monomers. NEB calculations were carried out to analyze the C-C coupling determining an elementary step and an activation energy of 1.07 eV was found. While nc-AFM is commonly employed to identify organic species on surfaces after reaction, high-speed variable temperature STM at the temperature close to the reaction on-set provides unique insights into the reaction dynamics that significantly improve DFT modelling. As such, it is a complementary tool that can be used to reveal the molecular dynamics of surface reactions and identify the catalytically active sites. These insights obtained from high-speed STM can help increase catalytic performance by improving understanding of the reaction and degradation mechanism of the catalyst, making this technique relevant to a variety of applications.

METHODS

All experiments were carried out under ultra-high vacuum (UHV) conditions with pressure in the 10^{-10} mbar regime. The precursor molecule, 1,4-dibromobenzene (98% purity), was acquired from Sigma-Aldrich. Precursors were dosed by a leak valve on Cu(110) held at room temperature. The substrate was prepared by repeated Ar+ sputtering (1.2 keV) and annealing (500 °C). STM experiments were performed with an Omicron variable temperature STM (VT-STM) operated by a R9plus controller (RHK Technology). Conventional STM scanning was performed in constant current mode. An add-on FAST module was used to achieve high frame acquisition speed (10 Hz) in a quasi-constant height mode, which can slightly change the appearance of surface structures compared to the constant current mode employed by slow scanning STM.[34] Raw FAST time series were initially processed through a dedicated Python package.[47]

Density functional theory (DFT) calculations were performed using the Vienna Ab initio Simulation Package (VASP). Plane-wave DFT calculations were performed using the Perdew-Burke-Ernzerhof[48] generalized-gradient approximation (PBE-GGA) for exchange-correlation potential, the projector augmented wave method,[49] and a basis set with an energy cut-off of 450 eV. The zero-damping DFT-D3 method of Grimme et al. was used for van der Waals correction of potential energy.[50] Cu(110) slabs were constructed using a lattice constant of 0.363 nm and a 1.8 nm vacuum layer, with five atomic layers and the positions of atoms in the bottom two layers fixed. OM chains were modelled with an epitaxy matrix of (2, 2 |−4, 9). Formation energy values were calculated using the following formula:

$$E_{form} = \frac{1}{n}\left[E_{tot}^{Cu110+n\ mol} - \left(E_{tot}^{Cu110} + n \cdot E_{tot}^{mol} + m \cdot E_{tot}^{Cu}\right)\right] \quad (1)$$

where $E_{tot}^{Cu_{110}+n\ mol}$, $E_{tot}^{Cu_{110}}$, E_{tot}^{mol} and E_{tot}^{Cu} are the total energies of the combined system, the Cu(110) substrate, the adsorbed molecules and the Cu adatoms. *n* and *m* are the number of phenylenes and Cu adatoms per unit cell, respectively. The energy of the Cu adatom is estimated by

$$E_{tot}^{Cu} = E_{tot}^{Cu/Cu(110)} - E_{tot}^{Cu_{110}} \quad (2)$$

$E_{tot}^{Cu/Cu(110)}$ is the energy of an isolated adatom on Cu(110). Geometry optimizations were carried out with a 5x5x1 k-mesh until the force on each atom is below 0.02 eV/Å. Interaction energies were calculated using the following formular: $E_i = E_{system} + E_{slab} - (E_{slab,OM\ monomer} + E_{slab,Br})$, where E_{system}, E_{slab}, $E_{slab,OM\ monomer}$ and $E_{slab,Br}$ are the energies of the total combined system, of the Cu(110) slab, of the OM monomer on the Cu(110) slab and of the Br atoms adsorbed on the Cu(110) slab. The energy of the formation of a Cu adatom from a perfect surface was calculated as the energy difference between a perfect surface and a surface with an adatom vacancy pair. NEB calculations were carried out with eight intermediate images and a force convergence criteria of 0.02 eV/Å on each atom. Quantification of the diffusion barriers were carried out at the Γ-point. The polymerization process was modelled with five separate NEB calculations and a 3x3x1 k-mesh. STM simulations were performed with a 5x5x1 k-point mesh. Images of the calculated structures were generated using the VMD software[51] and STM images were simulated via the Tersoff−Hamann approximation[52] using the calculated wave function of the relaxed structures obtained from VASP and visualized using the Hive software.[53]

ACKNOWLEDGMENTS

This work was partially supported by the project Grande Rilevanza Italy-Quebec of the Italian Ministero degli Affari Esteri e della Cooperazione Internazionale (MAECI), Direzione Generale per la Promozione del Sistema Paese and the project P2DAME “Gruppi di Ricerca 2020” of the Regione Lazio (Italy). This project has received funding from the European Union’s Horizon 2020 research and innovation programme under grant agreement No 654360 having benefited from the access provided by IOM-CNR in Trieste (Italy) within the framework of the NFFA-Europe Transnational Access Activity, proposal ID926. Computations were performed on the Graham cluster of the Shared Hierarchical Academic Research Computing Network (www.sharcnet.ca) and the Niagara supercomputer at the SciNet HPC Consortium, funded by the Canada Foundation for Innovation under Compute Canada, the Government of

Ontario, Ontario Research Fund-Research Excellence, and the University of Toronto. The authors acknowledge support from Digital Research Alliance of Canada (www.alliancecan.ca) for enabling the simulations. D.F.P. and F.R. acknowledge funding from NSERC (individual Discovery Grants) and from an FRQNT team grant.

REFERENCES

(1) Galeotti, G.; De Marchi, F.; Hamzehpoor, E.; MacLean, O.; Rajeswara Rao, M.; Chen, Y.; Besteiro, L. V.; Dettmann, D.; Ferrari, L.; Frezza, F.; Sheverdyaeva, P. M.; Liu, R.; Kundu, A. K.; Moras, P.; Ebrahimi, M.; Gallagher, M. C.; Rosei, F.; Perepichka, D. F.; Contini, G. Synthesis of mesoscale ordered two-dimensional π-conjugated polymers with semiconducting properties. *Nat. Mater.* **2020**, *19* (8), 874-880. DOI: 10.1038/s41563-020-0682-z.

(2) Mishra, S.; Beyer, D.; Eimre, K.; Kezilebieke, S.; Berger, R.; Gröning, O.; Pignedoli, C. A.; Müllen, K.; Liljeroth, P.; Ruffieux, P.; Feng, X.; Fasel, R. Topological frustration induces unconventional magnetism in a nanographene. *Nat. Nanotechnol.* **2020**, *15* (1), 22-28. DOI: 10.1038/s41565-019-0577-9.

(3) Rizzo, D. J.; Veber, G.; Cao, T.; Bronner, C.; Chen, T.; Zhao, F.; Rodriguez, H.; Louie, S. G.; Crommie, M. F.; Fischer, F. R. Topological band engineering of graphene nanoribbons. *Nature* **2018**, *560* (7717), 204-208. DOI: 10.1038/s41586-018-0376-8.

(4) Zhong, Y.; Cheng, B.; Park, C.; Ray, A.; Brown, S.; Mujid, F.; Lee, J.-U.; Zhou, H.; Suh, J.; Lee, K.-H.; Mannix, A. J.; Kang, K.; Sibener, S. J.; Muller, D. A.; Park, J. Wafer-scale synthesis of monolayer two-dimensional porphyrin polymers for hybrid superlattices. *Science* **2019**, *366* (6471), 1379. DOI: 10.1126/science.aax9385.

(5) Di Giovannantonio, M.; Kosmala, T.; Bonanni, B.; Serrano, G.; Zema, N.; Turchini, S.; Catone, D.; Wandelt, K.; Pasini, D.; Contini, G.; Goletti, C. Surface−Enhanced Polymerization via Schiff-Base Coupling at the Solid–Water Interface under pH Control. *J. Phys. Chem. C* **2015**, *119* (33), 19228-19235. DOI: 10.1021/acs.jpcc.5b05547.

(6) Cai, Z.-F.; Zhan, G.; Daukiya, L.; Eyley, S.; Thielemans, W.; Severin, K.; De Feyter, S. Electric-Field-Mediated Reversible Transformation between Supramolecular Networks and Covalent Organic Frameworks. *J. Am. Chem. Soc.* **2019**, *141* (29), 11404-11408. DOI: 10.1021/jacs.9b05265.

(7) Blunt, M. O.; Russell, J. C.; Champness, N. R.; Beton, P. H. Templating molecular adsorption using a covalent organic framework. *Chem. Commun.* **2010**, *46* (38), 7157-7159, 10.1039/C0CC01810D. DOI: 10.1039/C0CC01810D.

(8) Weiss, P. S.; Kamna, M. M.; Graham, T. M.; Stranick, S. J. Imaging Benzene Molecules and Phenyl Radicals on Cu{111}. *Langmuir* **1998**, *14* (6), 1284-1289. DOI: 10.1021/la970736i.

(9) Pham, T. A.; Tran, B. V.; Nguyen, M.-T.; Stöhr, M. Chiral-Selective Formation of 1D Polymers Based on Ullmann-Type Coupling: The Role of the Metallic Substrate. *Small* **2017**, *13* (13), 1603675. DOI: https://doi.org/10.1002/smll.201603675.

(10) Wang, T.; Huang, J.; Lv, H.; Fan, Q.; Feng, L.; Tao, Z.; Ju, H.; Wu, X.; Tait, S. L.; Zhu, J. Kinetic Strategies for the Formation of Graphyne Nanowires via Sonogashira Coupling on Ag(111). *J. Am. Chem. Soc.* **2018**, *140* (41), 13421-13428. DOI: 10.1021/jacs.8b08477.

(11) Wang, C.; Chi, L.; Ciesielski, A.; Samorì, P. Chemical Synthesis at Surfaces with Atomic Precision: Taming Complexity and Perfection. *Angew. Chem. Int. Ed.* **2019**, *58* (52), 18758-18775. DOI: https://doi.org/10.1002/anie.201906645.

(12) Dettmann, D.; Sheverdyaeva, P. M.; Hamzehpoor, E.; Franchi, S.; Galeotti, G.; Moras, P.; Ceccarelli, C.; Perepichka, D. F.; Rosei, F.; Contini, G. Electronic Band Engineering of Two-Dimensional Kagomé Polymers. *ACS Nano* **2024**, *18* (1), 849-857. DOI: 10.1021/acsnano.3c09476.

(13) Lackinger, M. Surface-assisted Ullmann coupling. *Chem. Commun.* **2017**, *53* (56), 7872-7885, 10.1039/C7CC03402D. DOI: 10.1039/C7CC03402D.

(14) Lipton-Duffin, J. A.; Ivasenko, O.; Perepichka, D. F.; Rosei, F. Synthesis of Polyphenylene Molecular Wires by Surface-Confined Polymerization. *Small* **2009**, *5* (5), 592-597, https://doi.org/10.1002/smll.200801943. DOI: https://doi.org/10.1002/smll.200801943.

(15) Eichhorn, J.; Nieckarz, D.; Ochs, O.; Samanta, D.; Schmittel, M.; Szabelski, P. J.; Lackinger, M. On-Surface Ullmann Coupling: The Influence of Kinetic Reaction Parameters on the Morphology and Quality of Covalent Networks. *ACS Nano* **2014**, *8* (8), 7880-7889. DOI: 10.1021/nn501567p.

(16) Wang, C.-X.; Chen, J.-L.; Shu, C.-H.; Shi, K.-J.; Liu, P.-N. On-surface synthesis of 2D COFs on Cu(111) via the formation of thermodynamically stable organometallic networks as the template.

Phys. Chem. Chem. Phys. **2019**, *21* (24), 13222-13229, 10.1039/C9CP01843C. DOI: 10.1039/C9CP01843C.
(17) Xi, M.; Bent, B. E. Mechanisms of the Ullmann coupling reaction in adsorbed monolayers. *J. Am. Chem. Soc.* **1993**, *115* (16), 7426-7433. DOI: 10.1021/ja00069a048.
(18) Albrecht, F.; Fatayer, S.; Pozo, I.; Tavernelli, I.; Repp, J.; Peña, D.; Gross, L. Selectivity in single-molecule reactions by tip-induced redox chemistry. *Science* **2022**, *377* (6603), 298-301. DOI: 10.1126/science.abo6471.
(19) Mishra, S.; Fatayer, S.; Fernández, S.; Kaiser, K.; Peña, D.; Gross, L. Nonbenzenoid High-Spin Polycyclic Hydrocarbons Generated by Atom Manipulation. *ACS Nano* **2022**, *16* (2), 3264-3271. DOI: 10.1021/acsnano.1c11157.
(20) Castro-Esteban, J.; Albrecht, F.; Fatayer, S.; Pérez, D.; Gross, L.; Peña, D. An on-surface Diels–Alder reaction. *Angewandte Chemie International Edition* **2021**, *60* (50), 26346-26350. DOI: https://doi.org/10.1002/anie.202110311.
(21) Ruan, Z.; Li, B.; Lu, J.; Gao, L.; Sun, S.; Zhang, Y.; Cai, J. Real-space imaging of a phenyl group migration reaction on metal surfaces. *Nat. Commun.* **2023**, *14* (1), 970. DOI: 10.1038/s41467-023-36696-6.
(22) Dettmann, D.; Galeotti, G.; MacLean, O.; Tomellini, M.; Di Giovannantonio, M.; Lipton-Duffin, J.; Verdini, A.; Floreano, L.; Fagot-Revurat, Y.; Perepichka, D. F.; Rosei, F.; Contini, G. Identification of Topotactic Surface-Confined Ullmann-Polymerization. *Small* **2021**, *17* (41), 2103044, https://doi.org/10.1002/smll.202103044. DOI: https://doi.org/10.1002/smll.202103044.
(23) Galeotti, G.; Di Giovannantonio, M.; Lipton-Duffin, J.; Ebrahimi, M.; Tebi, S.; Verdini, A.; Floreano, L.; Fagot-Revurat, Y.; Perepichka, D. F.; Rosei, F.; Contini, G. The role of halogens in on-surface Ullmann polymerization. *Faraday Discuss.* **2017**, *204* (0), 453-469, 10.1039/C7FD00099E. DOI: 10.1039/C7FD00099E.
(24) Di Giovannantonio, M.; Tomellini, M.; Lipton-Duffin, J.; Galeotti, G.; Ebrahimi, M.; Cossaro, A.; Verdini, A.; Kharche, N.; Meunier, V.; Vasseur, G.; Fagot-Revurat, Y.; Perepichka, D. F.; Rosei, F.; Contini, G. Mechanistic Picture and Kinetic Analysis of Surface-Confined Ullmann Polymerization. *J. Am. Chem. Soc.* **2016**, *138* (51), 16696-16702. DOI: 10.1021/jacs.6b09728.
(25) Abadía, M.; Ilyn, M.; Piquero-Zulaica, I.; Gargiani, P.; Rogero, C.; Ortega, J. E.; Brede, J. Polymerization of Well-Aligned Organic Nanowires on a Ferromagnetic Rare-Earth Surface Alloy. *ACS Nano* **2017**, *11* (12), 12392-12401. DOI: 10.1021/acsnano.7b06374.
(26) Di Giovannantonio, M.; Contini, G. Reversibility and intermediate steps as key tools for the growth of extended ordered polymers via on-surface synthesis. *J. Phys. Condens. Matter* **2018**, *30* (9), 093001. DOI: 10.1088/1361-648x/aaa8cb.
(27) Grossmann, L.; Hocke, M.; Galeotti, G.; Contini, G.; Floreano, L.; Cossaro, A.; Ghosh, A.; Schmittel, M.; Rosen, J.; Heckl, W. M.; Björk, J.; Lackinger, M. Mechanistic Insights into On-Surface Reactions from Isothermal Temperature-Programmed X-ray Photoelectron Spectroscopy. *Nanoscale* **2024**, 10.1039/D4NR00468J. DOI: 10.1039/D4NR00468J.
(28) Lackinger, M. Possibilities and Limitations of Kinetic Studies in On-Surface Synthesis by Real Time X-ray Photoelectron Spectroscopy. *ChemPhysChem* **2024**, e202400156. DOI: https://doi.org/10.1002/cphc.202400156.
(29) Bieri, M.; Nguyen, M.-T.; Gröning, O.; Cai, J.; Treier, M.; Aït-Mansour, K.; Ruffieux, P.; Pignedoli, C. A.; Passerone, D.; Kastler, M.; Müllen, K.; Fasel, R. Two-Dimensional Polymer Formation on Surfaces: Insight into the Roles of Precursor Mobility and Reactivity. *J. Am. Chem. Soc.* **2010**, *132* (46), 16669-16676. DOI: 10.1021/ja107947z.
(30) Fritton, M.; Duncan, D. A.; Deimel, P. S.; Rastgoo-Lahrood, A.; Allegretti, F.; Barth, J. V.; Heckl, W. M.; Björk, J.; Lackinger, M. The Role of Kinetics versus Thermodynamics in Surface-Assisted Ullmann Coupling on Gold and Silver Surfaces. *J. Am. Chem. Soc.* **2019**, *141* (12), 4824-4832. DOI: 10.1021/jacs.8b11473.
(31) Zhang, Z.; Perepichka, D. F.; Khaliullin, R. Z. Adatoms in the Surface-Confined Ullmann Coupling of Phenyl Groups. *J. Phys. Chem. Lett.* **2021**, 11061-11069. DOI: 10.1021/acs.jpclett.1c02914.

(32) Patera, L. L.; Zou, Z.; Dri, C.; Africh, C.; Repp, J.; Comelli, G. Imaging on-surface hierarchical assembly of chiral supramolecular networks. *Phys. Chem. Chem. Phys.* **2017**, *19* (36), 24605-24612, 10.1039/C7CP01341H. DOI: 10.1039/C7CP01341H.
(33) Patera, L. L.; Bianchini, F.; Africh, C.; Dri, C.; Soldano, G.; Mariscal, M. M.; Peressi, M.; Comelli, G. Real-time imaging of adatom-promoted graphene growth on nickel. *Science* **2018**, *359* (6381), 1243. DOI: 10.1126/science.aan8782.
(34) Dri, C.; Panighel, M.; Tiemann, D.; Patera, L. L.; Troiano, G.; Fukamori, Y.; Knoller, F.; Lechner, B. A. J.; Cautero, G.; Giuressi, D.; Comelli, G.; Fraxedas, J.; Africh, C.; Esch, F. The new FAST module: A portable and transparent add-on module for time-resolved investigations with commercial scanning probe microscopes. *Ultramicroscopy* **2019**, *205*, 49-56. DOI: https://doi.org/10.1016/j.ultramic.2019.05.010.
(35) Rahn, B.; Magnussen, O. M. Formation and Diffusion of Subsurface Adsorbates at Electrodes. *J. Am. Chem. Soc.* **2018**, *140* (29), 9066-9069. DOI: 10.1021/jacs.8b04903.
(36) Matsushima, H.; Taranovskyy, A.; Haak, C.; Gründer, Y.; Magnussen, O. M. Reconstruction of Cu(100) Electrode Surfaces during Hydrogen Evolution. *J. Am. Chem. Soc.* **2009**, *131* (30), 10362-10363. DOI: 10.1021/ja904033t.
(37) Rahn, B.; Wen, R.; Deuchler, L.; Stremme, J.; Franke, A.; Pehlke, E.; Magnussen, O. M. Coadsorbate-Induced Reversal of Solid–Liquid Interface Dynamics. *Angew. Chem. Int. Ed.* **2018**, *57* (21), 6065-6068. DOI: https://doi.org/10.1002/anie.201712728.
(38) Guézo, S.; Taranovskyy, A.; Matsushima, H.; Magnussen, O. M. Surface Dynamics of Lead Adsorbates at the Cu(100)–Electrolyte Interface. *J. Phys. Chem. C* **2011**, *115* (39), 19336-19342. DOI: 10.1021/jp2079988.
(39) Tansel, T.; Magnussen, O. M. Video STM Studies of Adsorbate Diffusion at Electrochemical Interfaces. *Phys. Rev. Lett.* **2006**, *96* (2), 026101. DOI: 10.1103/PhysRevLett.96.026101.
(40) Grill, L.; Hecht, S. Covalent on-surface polymerization. *Nat. Chem.* **2020**, *12* (2), 115-130. DOI: 10.1038/s41557-019-0392-9.
(41) Galeotti, G.; Di Giovannantonio, M.; Cupo, A.; Xing, S.; Lipton-Duffin, J.; Ebrahimi, M.; Vasseur, G.; Kierren, B.; Fagot-Revurat, Y.; Tristant, D.; Meunier, V.; Perepichka, D. F.; Rosei, F.; Contini, G. An unexpected organometallic intermediate in surface-confined Ullmann coupling. *Nanoscale* **2019**, *11* (16), 7682-7689, 10.1039/C9NR00672A. DOI: 10.1039/C9NR00672A.
(42) Di Giovannantonio, M.; El Garah, M.; Lipton-Duffin, J.; Meunier, V.; Cardenas, L.; Fagot Revurat, Y.; Cossaro, A.; Verdini, A.; Perepichka, D. F.; Rosei, F.; Contini, G. Insight into Organometallic Intermediate and Its Evolution to Covalent Bonding in Surface-Confined Ullmann Polymerization. *ACS Nano* **2013**, *7* (9), 8190-8198. DOI: 10.1021/nn4035684.
(43) Di Giovannantonio, M.; El Garah, M.; Lipton-Duffin, J.; Meunier, V.; Cardenas, L.; Fagot-Revurat, Y.; Cossaro, A.; Verdini, A.; Perepichka, D. F.; Rosei, F.; Contini, G. Reply to "Comment on 'Insight into Organometallic Intermediate and Its Evolution to Covalent Bonding in Surface-Confined Ullmann Polymerization'". *ACS Nano* **2014**, *8* (3), 1969-1971. DOI: 10.1021/nn500322r.
(44) Karimi, M.; Tomkowski, T.; Vidali, G.; Biham, O. Diffusion of Cu on Cu surfaces. *Physical Review B* **1995**, *52* (7), 5364-5374. DOI: 10.1103/PhysRevB.52.5364.
(45) Zhang, D.; Wang, G.; Chen, C.; Joshi, T.; Chen, X.-K.; Evans, A. M.; Matsumoto, M.; Dichtel, W. R.; Li, H.; Crommie, M. F.; Brédas, J.-L. Mechanism of Formation of Benzotrithiophene-Based Covalent Organic Framework Monolayers on Coinage-Metal Surfaces: C–C Coupling Selectivity and Monomer–Metal Interactions. *Chem. Mater.* **2020**, *32* (24), 10688-10696. DOI: 10.1021/acs.chemmater.0c03901.
(46) Björk, J.; Sánchez-Sánchez, C.; Chen, Q.; Pignedoli, C. A.; Rosen, J.; Ruffieux, P.; Feng, X.; Narita, A.; Müllen, K.; Fasel, R. The Role of Metal Adatoms in a Surface-Assisted Cyclodehydrogenation Reaction on a Gold Surface. *Angew. Chem. Int. Ed.* **2022**, *61* (49), e202212354. DOI: https://doi.org/10.1002/anie.202212354.
(47) Briegel, K. D.; Riccius, F.; Filser, J.; Bourgund, A.; Spitzenpfeil, R.; Panighel, M.; Dri, C.; Lechner, B. A. J.; Esch, F. PyfastSPM: A Python package to convert 1D FastSPM data streams into publication quality movies. *SoftwareX* **2023**, *21*, 101269. DOI: https://doi.org/10.1016/j.softx.2022.101269.

(48) Perdew, J. P.; Ernzerhof, M.; Burke, K. Rationale for mixing exact exchange with density functional approximations. *J. Chem. Phys.* **1996**, *105* (22), 9982-9985. DOI: 10.1063/1.472933.
(49) Kresse, G.; Joubert, D. From ultrasoft pseudopotentials to the projector augmented-wave method. *Phys. Rev. B* **1999**, *59* (3), 1758-1775. DOI: 10.1103/PhysRevB.59.1758.
(50) Grimme, S.; Antony, J.; Ehrlich, S.; Krieg, H. A consistent and accurate ab initio parametrization of density functional dispersion correction (DFT-D) for the 94 elements H-Pu. *J. Chem. Phys.* **2010**, *132* (15), 154104. DOI: 10.1063/1.3382344.
(51) Humphrey, W.; Dalke, A.; Schulten, K. VMD: visual molecular dynamics. *J. Mol. Graph.* **1996**, *14* (1), 33-38.
(52) Tersoff, J.; Hamann, D. R. Theory of the scanning tunneling microscope. *Phys. Rev. B* **1985**, *31* (2), 805-813. DOI: 10.1103/PhysRevB.31.805.
(53) Vanpoucke, D. E. P.; Brocks, G. Formation of Pt-induced Ge atomic nanowires on Pt/Ge(001): A density functional theory study. *Phys. Rev. B* **2008**, *77* (24), 241308. DOI: 10.1103/PhysRevB.77.241308.